

# Probing magnetic order and disorder in the one-dimensional molecular spin chains $\text{CuF}_2(\text{pyz})$ and $[\text{Ln}(\text{hfac})_3(\text{boaDTDA})]_n$ ( $\text{Ln} = \text{Sm}, \text{La}$ ) using implanted muons

T. Lancaster<sup>1</sup>, B.M. Huddart<sup>1</sup>, R.C. Williams<sup>1,2</sup>, F. Xiao<sup>1,3,4</sup>,  
K.J.A. Franke<sup>1,5,6</sup>, P.J. Baker<sup>7</sup>, F.L. Pratt<sup>7</sup>, S.J. Blundell<sup>8</sup>, J.A.  
Schlueter<sup>9,10</sup>, M.B. Mills<sup>11</sup>, A.C. Maahs<sup>11</sup> and K.E. Preuss<sup>11</sup>

<sup>1</sup>Durham University, Centre for Materials Physics, Durham, DH1 3LE, United Kingdom

E-mail: tom.lancaster@durham.ac.uk

<sup>2</sup>Department of Physics, University of Warwick, Gibbet Hill Road, Coventry CV4 7AL, United Kingdom

<sup>3</sup>Department of Chemistry and Biochemistry, University of Bern, Freiestrasse 3, CH-3012 Bern, Switzerland

<sup>4</sup>Laboratory for Neutron Scattering and Imaging, Paul Scherrer Institut, CH-5232 Villigen PSI, Switzerland

<sup>5</sup>School of Physics and Astronomy, University of Leeds, Leeds LS2 9JT, United Kingdom

<sup>6</sup>Department of Materials Science and Engineering, University of California, Berkeley, Berkeley, California 94720, USA

<sup>7</sup>ISIS Facility, Rutherford Appleton Laboratory, Chilton, Didcot, OX11 0QX, United Kingdom

<sup>8</sup>Department of Physics, University of Oxford, Clarendon Laboratory, Parks Road, Oxford, OX1 3PU, United Kingdom

<sup>9</sup>Materials Science Division, Argonne National Laboratory, Argonne, Illinois 60439, USA

<sup>10</sup>Division of Materials Research, National Science Foundation, 2415 Eisenhower Ave, Alexandria, VA 22314, USA

<sup>11</sup>Department of Chemistry, University of Guelph, Guelph, Ontario N1G 2W1, Canada

**Abstract.** We present the results of muon-spin relaxation ( $\mu^+\text{SR}$ ) measurements on antiferromagnetic and ferromagnetic spin chains. In antiferromagnetic  $\text{CuF}_2(\text{pyz})$  we identify a transition to long range magnetic order taking place at  $T_N = 0.6(1)$  K, allowing us to estimate a ratio with the intrachain exchange of  $T_N/|J| \approx 0.1$  and the ratio of interchain to intrachain exchange coupling as  $|J'/J| \approx 0.05$ . The ferromagnetic chain  $[\text{Sm}(\text{hfac})_3(\text{boaDTDA})]_n$  undergoes an ordering transition at  $T_c = 2.8(1)$  K, seen via a broad freezing of dynamic fluctuations on the muon (microsecond) timescale and implying  $T_c/|J| \approx 0.6$ . The ordered radical moment continues to fluctuate on this timescale down to 0.3 K, while the Sm moments remain disordered. In contrast, the radical spins in  $[\text{La}(\text{hfac})_3(\text{boaDTDA})]_n$  remain magnetically disordered down to  $T = 0.1$  K suggesting  $T_c/|J| < 0.17$ .

*Keywords:* muon-spin relaxation, one-dimensional magnetism, radical magnetism

Submitted to: *J. Phys.: Condens. Matter*

## 1. Introduction

A major theme in the investigation of molecular magnets has concerned materials whose low-energy physics arises from interactions that are constrained to act in less than three spatial dimensions [1, 2]. This is achieved by linking localized spins using molecular ligands in such a way as to promote strong interactions between the magnetic centres only along particular directions, with weaker ones acting along others. Particularly notable is the one-dimensional (1D) spin chain, since an idealised version of this problem can be thoroughly described theoretically, revealing a rich range of correlations and an exotic spectrum of excitations [3]. Although an isolated one dimensional spin chain will not show any long-range magnetic order [4], real materials will host interactions between chains, however weak, which have a strong effect on their properties.

A quasi-one-dimensional Heisenberg magnet with principal exchange interaction  $J$  acting along the chains [5] and a smaller interaction  $J'$  linking the chains is described by the Hamiltonian [6]

$$\hat{H} = J \sum_{\langle ij \rangle} \hat{\mathbf{S}}_i \cdot \hat{\mathbf{S}}_j + J' \sum_{\langle ij' \rangle} \hat{\mathbf{S}}_i \cdot \hat{\mathbf{S}}_{j'}, \quad (1)$$

where the sum  $\langle ij \rangle$  is over nearest-neighbour spins on the same chain and  $i$  and  $j'$  label spins on adjacent chains. In order to probe 1D behavior in a system described by this model, we work in a temperature regime where  $|J'| \ll T \ll |J|$ . When we approach a regime where the characteristic energy of the thermal fluctuations allows detail at the scale of  $J'$  to be resolved, we should expect that the three-dimensional nature of the material becomes evident and it will magnetically order. However, the strongly anisotropic nature of the exchange ( $|J'/J| \ll 1$ ) will have consequences on the ordered state that arises [7] and the ordering temperature is driven downwards by the 1D nature of the system compared to a three-dimensional one. The ordered magnetic moments will also be renormalised [8], making them potentially very small, and difficult to observe with magnetic susceptibility measurements. Finite, but possibly very long, correlation lengths may exist above the ordering temperature, reducing the entropy in the system. Consequently, the entropy change on ordering will be much reduced compared to a more isotropic system and may prevent specific heat measurements from detecting a transition [7]. For this reason sensitive magnetic measurement techniques such as muon-spin relaxation ( $\mu^+$ SR) have found a use in detecting the transitions to long range magnetic order that allow us to quantify the strength of the interchain exchange and reveal how well real materials are described by idealised models [9, 6, 10]

In this paper we present  $\mu^+$ SR measurements on two different 1D coordination polymer systems: (i) the quasi-1D Heisenberg antiferromagnet  $\text{CuF}_2(\text{pyz})$ , built from

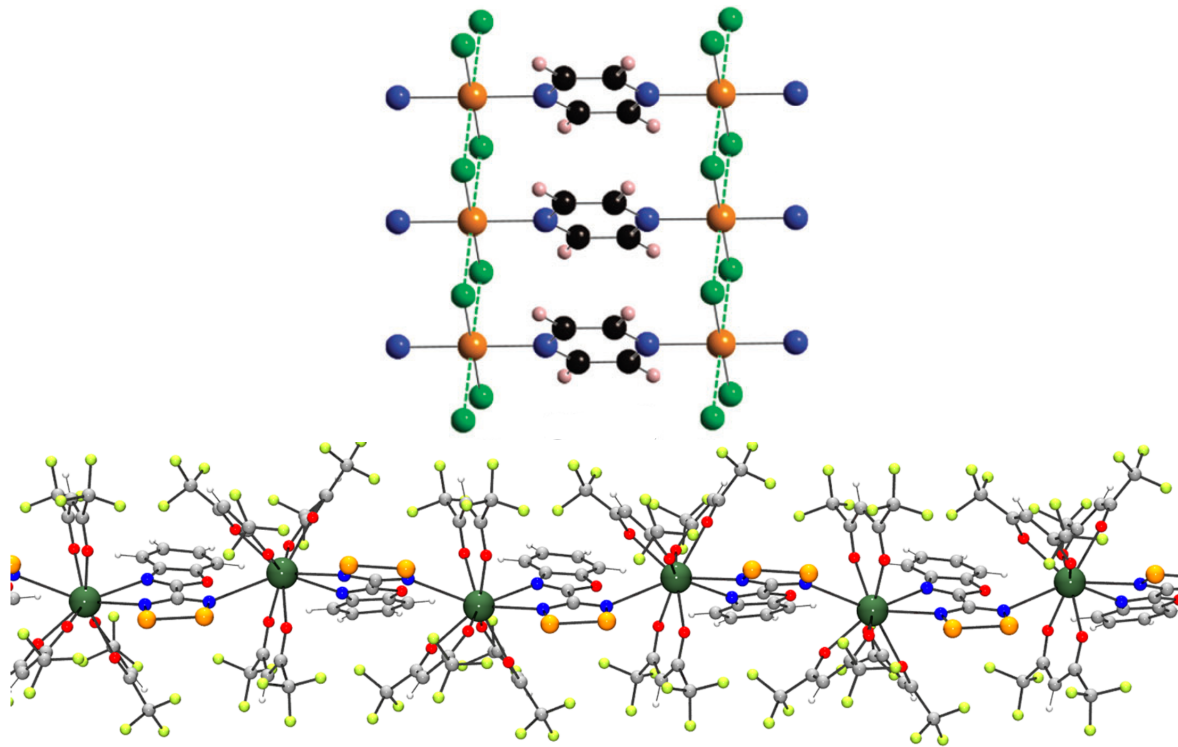


**Figure 1.** *Top:* structure of  $\text{CuF}_2(\text{pyz})$  with the strong antiferromagnetic coupling along the horizontal  $\text{Cu-pyz-Cu}$  chains [11] (black, C; blue N; pink H, orange Cu; green F). *Bottom:* structure of  $[\text{Ln}(\text{hfac})_3(\text{boaDTDA})]_n$ , where ferromagnetic coupling is mediated along the chains of  $\text{boaDTDA}$  radical ligands via the  $\text{Ln}(\text{hfac})_3$  units [13]. (dark green,  $\text{Ln}$ ; orange, S; red, O; grey, C; white, H; blue, N; pale green, F.)

$\text{Cu}^{2+}$  spins linked antiferromagnetically with pyrazine ( $\text{pyz} = \text{C}_4\text{H}_4\text{N}_2$ ) ligands [Fig. 1 (top)] [11]; (ii) a quasi-1D Heisenberg ferromagnetic series based on a  $-\text{[Ln}^{3+}\text{-radical}]_n-$  paradigm, namely  $[\text{Ln}(\text{hfac})_3(\text{boaDTDA})]_n$  [Fig. 1 (bottom)] where  $\text{Ln} = \text{Sm, La}$ ; ( $\text{boaDTDA}$ ) is the radical ligand 4-(benzoxazol-20-yl)-1,2,3,5-dithiadiazolyl and  $\text{hfac} = 1,1,1,5,5,5$ -hexafluoroacetylacetonato [12, 13]. In both systems, the muon relaxation is dominated by the magnetism of the nuclear spins in the high-temperature paramagnetic regime owing to the rapid fluctuations of the electronic spins on the timescale of muon spin precession. However, on cooling, as fluctuations in the electronic degrees of freedom slow and enter the muon time window, the nature of the muon coupling with the system changes and transitions to regimes of magnetic order are detected.

## 2. Experimental

In a  $\mu^+$ SR experiment [14] spin-polarized positive muons are stopped in a target sample, where the muon usually occupies an interstitial position in the crystal. The observed property in the experiment is the time evolution of the muon spin polarization, the behaviour of which depends on the local magnetic field at the muon site. Each muon

decays, with an average lifetime of  $2.2 \mu\text{s}$ , into two neutrinos and a positron, the latter particle being emitted preferentially along the instantaneous direction of the muon spin. Recording the time dependence of the positron emission directions therefore allows the determination of the spin-polarization of the ensemble of muons. In our experiments, positrons are detected by detectors placed forward (F) and backward (B) of the initial muon polarization direction. Histograms  $N_{\text{F}}(t)$  and  $N_{\text{B}}(t)$  record the number of positrons detected in the two detectors as a function of time following the muon implantation. The quantity of interest is the decay positron asymmetry function, defined as

$$A(t) = \frac{N_{\text{F}}(t) - \alpha_{\text{exp}} N_{\text{B}}(t)}{N_{\text{F}}(t) + \alpha_{\text{exp}} N_{\text{B}}(t)}, \quad (2)$$

where  $\alpha_{\text{exp}}$  is an experimental calibration constant.  $A(t)$  is proportional to the spin polarization of the muon ensemble.

Zero-field (ZF) muon-spin relaxation ( $\mu^+\text{SR}$ ) measurements were carried out on polycrystalline samples using the MuSR and HIFI spectrometers at the STFC-ISIS Facility, Rutherford Appleton Laboratory UK. For the measurements on  $\text{CuF}_2(\text{pyz})$ , a sample was packed in an Ag foil envelope (foil thickness  $12.5 \mu\text{m}$ ), and attached to the cold finger of a  $^3\text{He}$  cryostat. For measurements on  $[\text{Ln}(\text{hfac})_3(\text{boaDTDA})]_n$  samples were sealed in an Ag foil envelope inside an airtight sample holder and mounted on the cold finger of a dilution refrigerator.

### 3. One-dimensional antiferromagnetism in $\text{CuX}_2(\text{pyz})$

The isostructural series  $\text{CuX}_2(\text{pyz})$ , where  $X = \text{Br}, \text{Cl}, \text{F}$ , share a rectangular lattice structure composed of  $S = 1/2$  Heisenberg  $\text{Cu}^{2+}$  ions. The  $\text{Cu}^{2+}$  ions are linked into chains by bridging pyrazine molecules, which are themselves cross-linked via dihalide bridges to create 2D layers (Fig. 1, top). Antiferromagnetic superexchange pathways are therefore provided by both pyrazine and dihalide bridges, and interlayer magnetic coupling is small in comparison. For both  $X = \text{Br}$  and  $\text{Cl}$  materials, the largest exchange strength  $J = 46 \text{ K}$  ( $\text{Br}$ ) and  $= 28 \text{ K}$  ( $\text{Cl}$ ) was suggested to act along the halide bridges, with smaller exchange of around  $8 \text{ K}$  along the pyz chains [15]. Previous  $\mu^+\text{SR}$  investigations have determined transition temperatures for  $X = \text{Br}$  and  $\text{Cl}$  [16], yielding ratios of the ordering temperature to principal coupling of  $T_{\text{N}}/|J| \approx 0.08$  ( $\text{Br}$ ) and  $\approx 0.11$  ( $\text{Cl}$ ), although the significant value of the  $\text{Cu-pyz-Cu}$  coupling means that these systems are best regarded as rectangular lattice antiferromagnets. This coordination polymer family has more recently been extended to include the  $X = \text{F}$  system,  $\text{CuF}_2(\text{pyz})$  [11] which is notable for the small value of exchange coupling promoted along the fluorine bridges, estimated to be of order  $1 \text{ K}$ , while the principal exchange is along the  $\text{Cu-pyz-Cu}$  links and was estimated to be  $J = 7 \text{ K}$ , such that quasi-1D behaviour might be expected, with no magnetic transition identified down to  $T \approx 0.6 \text{ K}$ .

Example ZF  $\mu^+\text{SR}$  data for  $\text{CuF}_2(\text{pyz})$  are shown in Fig. 2(a), where oscillations are seen at all measured temperatures. The low frequency oscillations for  $T > 0.6 \text{ K}$

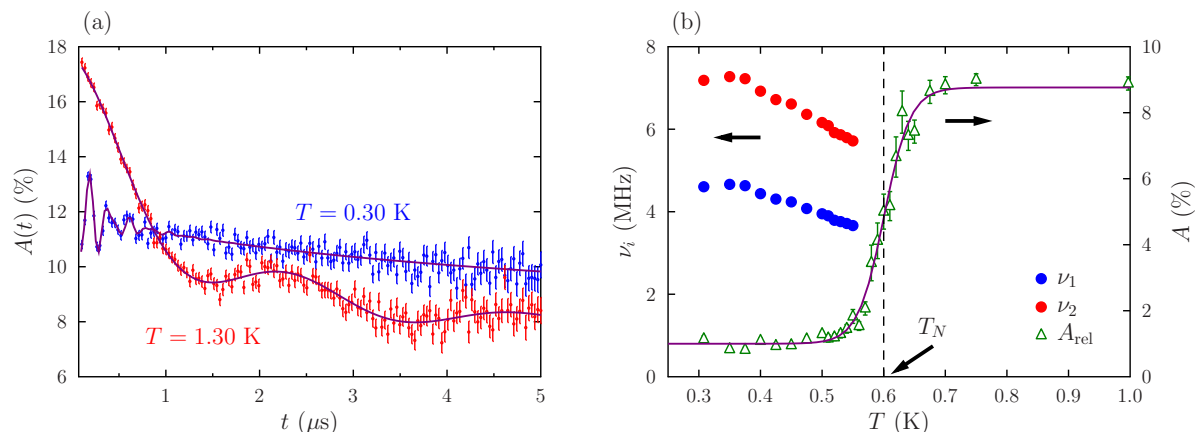


**Figure 2.** (a) ZF data measured on  $\text{CuF}_2(\text{pyz})$  above and below  $T_N$ . (b) Temperature evolution of (*left axis*) precession frequencies and (*right axis*) relaxing amplitude  $A_{\text{rel}}$ .

are common in fluorine-containing materials and are caused by dipole-dipole coupling between the muon and fluorine nuclei [17, 18]. These oscillations are typically resolved in the paramagnetic regime of molecular magnets of this type since, in this regime, the electronic moments on the  $\text{Cu}^{2+}$  ions fluctuate rapidly on the muon (microsecond) timescale and are motionally narrowed from the spectrum, leaving the quasistatic nuclear moments to relax the muon spins [19]. The data were found to be best described by the oscillations characteristic of the bound state of a  $\mu^+$  and a single F ion, and were fitted to a function of the form

$$A(t) = A_1 D(t) e^{-\lambda_1 t} + A_2 \exp^{-\sigma^2 t^2} + A_{\text{bg}} e^{-\lambda_{\text{bg}} t}, \quad (3)$$

where the first term represents the contribution from muons strongly coupled to fluorine nuclei, the second to muons coupled to a distribution of other quasistatic nuclei and the third term accounts for muons that implant in the sample holder. In Eqn (3),  $D(t)$  accounts for the muon-fluorine coupling, which takes the form [17]

$$D(t) = \frac{1}{6} \left[ 1 + 2 \cos\left(\frac{\omega t}{2}\right) + \cos(\omega t) + 2 \cos\left(\frac{3\omega t}{2}\right) \right], \quad (4)$$

where  $\omega = \mu_0 \gamma_\mu \gamma_F \hbar / 4\pi r^3$ ,  $\gamma_i$  are gyromagnetic ratios and  $r$  is the muon-fluorine distance. The fitted value of  $\omega = 1.74(2) \mu\text{s}^{-1}$  corresponds to a muon-fluorine separation of  $r = 1.09(1) \text{ \AA}$ . (This value represents a time-averaged bond length, as the frequencies of vibrational modes exceed those accessible by  $\mu^+$ SR.) It is therefore likely that one class of muon sites occurs near the fluorine nuclei and contributes the component with amplitude  $A_1$  in Eqn (3), while another couples closer to the pyz groups, giving rise to the component with amplitude  $A_2$ . This is consistent with the behaviour usually seen in materials of this type [20] and with computations of the muon sites using electronic structure methods [21].

The more rapid oscillations measured for  $T < 0.5$  K are characteristic of a quasistatic local magnetic field at the muon stopping site caused by long range magnetic

order [20]. This causes a coherent precession of the spins of those muons with a component of their spin polarization perpendicular to this local field. The frequencies of the oscillations are given by  $\nu_i = \gamma_\mu B_i / 2\pi$ , where  $\gamma_\mu$  is the muon gyromagnetic ratio ( $= 2\pi \times 135.5 \text{ MHz T}^{-1}$ ) and  $B_i$  is the average magnitude of the local magnetic field at the  $i$ th muon site. This is indicative of long-range magnetic order of the  $\text{Cu}^{2+}$  ions, and also implies the existence of two magnetically inequivalent muon stopping sites. Asymmetry spectra were fitted to damped cosinusoidal functions [ $A_i e^{-\lambda_i t} \cos(2\pi\nu_i t + \phi_i)$ , where  $\phi_i$  is a phase offset and  $\lambda_i$  a relaxation rate] and the temperature dependence of the two resolvable precession frequencies are shown in Fig. 2(b), where their relative magnitudes were held in fixed proportion. As was found in the  $X = \text{Br}$  and  $\text{Cl}$  materials [16], the oscillations become heavily damped and therefore unresolvable as the magnetic transition is approached from below. This effect means that frequencies cannot be reliably fitted close to the Néel temperature  $T_N$ . Instead, data were binned heavily (in order to smooth out the oscillations) and fitted to a purely decaying asymmetry relaxation function  $A_{\text{rel}} \exp(-\lambda t)$ . A significant change is visible in the relaxing amplitude  $A_{\text{rel}}$  [Fig. 2(b)], which allows us to estimate  $T_N = 0.6(1) \text{ K}$ . (This step change in relaxing amplitude reflects a fraction of lost asymmetry within the ordered state, where large, static or slowly fluctuating internal magnetic fields lead to rapid precession outside of the resolution limit set by the muon pulse width, and therefore tracks the evolution of static internal fields in the sample.)

A useful figure of merit in comparing the success with which a material realizes one-dimensionality is  $T_N/|J|$ , as this quantity should be zero in the ideal case and close to unity for an isotropic material. This quantity may also be used to estimate  $J'$ , which is the parameter of interest in the Hamiltonian in Eqn (1). One method of doing this in antiferromagnetic chains has been developed from Quantum Monte Carlo computations [22], whose results may be approximated using the expression

$$|J'|/k_B = \frac{T_N}{4c \sqrt{\ln\left(\frac{a|J|}{k_B T_N}\right) + \frac{1}{2} \ln \ln\left(\frac{a|J|}{k_B T_N}\right)}}, \quad (5)$$

with  $a = 2.6$  and  $c = 0.233$ . This yields a value of  $|J'/J| \approx 0.05$  (assuming  $J = 7 \text{ K}$ ), suggesting it is a reasonable approximation of a 1D Heisenberg antiferromagnet, comparable in the isolation of its chains with  $\text{KCuF}_3$  [6]‡. The exchange  $J'$  represents an effective geometric average over the three-dimensional exchange couplings in the lattice, but which will be dominated in this case by the coupling along the fluorine bibridges. As a result, this value is consistent with the estimate of 1 K coupling though these links made from the susceptibility data [11]. In addition, coupled chain mean field theory [8] predicts an ordered moment of  $\approx 0.2 \mu_B$ , consistent with the muon precession frequencies measured.

‡ Note that there is an error in the expression in Eqn (5) in Refs. [1] and [6], where the square root in the denominator has been omitted.

#### 4. One-dimensional ferromagnetism in $[Ln(\text{hfac})_3(\text{boaDTDA})]_n$ , $Ln = \text{Sm}, \text{La}$

The  $-[(\text{metal})^{3+} - (\text{radical})]-$  series  $[Ln(\text{hfac})_3(\text{boaDTDA})]_n$ , was the first reported coordination polymer including a bridging DTDA (-1,2,3,5-dithiadiazolyl) radical ligand [12]. The structure is formed from  $Ln^{3+}(\text{hfac})_3$  units arranged along the crystallographic  $b$ -direction, linked with  $S = 1/2$  radical boaDTDA ligands (Fig. 1, bottom). The 1D chains pack such that the heteroatoms of the boaDTDA ligands do not allow any close contacts between chains [12, 13]. Materials with  $Ln = \text{La}$  and  $\text{Sm}$  were both found to show 1D ferromagnetic exchange interactions between the radical spins, mediated via the  $Ln^{3+}$  ions [12, 13]. Such FM exchange can be achieved if there is a different symmetry between the magnetic orbital of each radical and the orbitals of the bridging species with which it overlaps. This is the case here owing to the  $\approx 30^\circ$  angle between the planes of the radical species on each side of the bridging ion [12].

Results of room temperature magnetometry in the  $Ln = \text{La}$  material [12] are consistent with a diamagnetic  $\text{La}^{3+}$  metal ion ( $4f^0$ ) and one  $S = 1/2$  spin per radical unit. Low temperature susceptibility measurements showed FM interactions which have principal ferromagnetic exchange strength of  $J = -0.58$  K. The dc magnetic susceptibility of the  $Ln = \text{Sm}$  material [13] is consistent with the expected behaviour of one  $\text{Sm}^{3+}$  metal ion ( $4f^5$ ,  $g_J J = 0.71$ ) and one  $S_{\text{rad}} = 1/2$  boaDTDA radical ( $g_J J = 1$ ) per repeat unit. Again, low temperature dc susceptibility suggests ferromagnetic interactions with exchange constant  $J = -4.4(2)$  K. Notably, below  $T = 3.1$  K, the magnetic susceptibility in the  $Ln = \text{Sm}$  material becomes strongly magnetic field-dependent, suggesting the stabilisation of a ferromagnetically ordered state. The magnetic order was suggested to involve the larger radical spins only, with the  $\text{Sm}^{3+}$  spins apparently remaining disordered down to  $T = 2$  K.

The FM interchain coupling in the  $\text{Sm}$  system was explained using the McConnell I mechanism [13, 23]. Here FM coupling between net magnetic moments on large molecules can occur via the contact between  $\alpha$  (positive, up) spin density on one molecule and  $\beta$  (negative, down) spin density on its neighbour. When the dominant contact is between  $\alpha$  and  $\beta$  it results in antiparallel alignment of these moments, and therefore alignment between the majority  $\alpha$  components and overall FM coupling.

ZF  $\mu^+$ SR measurements of the  $Ln = \text{Sm}$  material were made at temperatures between  $T = 0.2$  K and 20 K. Example spectra measured at three different temperatures are shown in Fig. 3. The spectra at temperatures  $> 4$  K exhibit a low frequency oscillation that looks intermediate in character between the F- $\mu^+$  oscillations seen for  $\text{CuF}_2(\text{pyz})$  and a Kubo-Toyabe (KT) function. The KT function  $[D(t) = \frac{1}{3} + \frac{2}{3}(1 - \Delta^2 t^2) \exp(-\Delta^2 t^2/2)]$  results from the coupling of muons to a dense, classical distribution of random, static moments with magnitudes centred around zero, which gives rise to a variance in the magnetic field distribution at the muon site of  $\Delta^2 = \gamma_\mu^2 \langle B^2 \rangle$ . In contrast, the muon-dipole coupling discussed above models the quantum mechanical interaction of a small number of moments. The intermediate nature of the relaxation seen here, is consistent with the muon spin being relaxed by several nuclear moments localized close

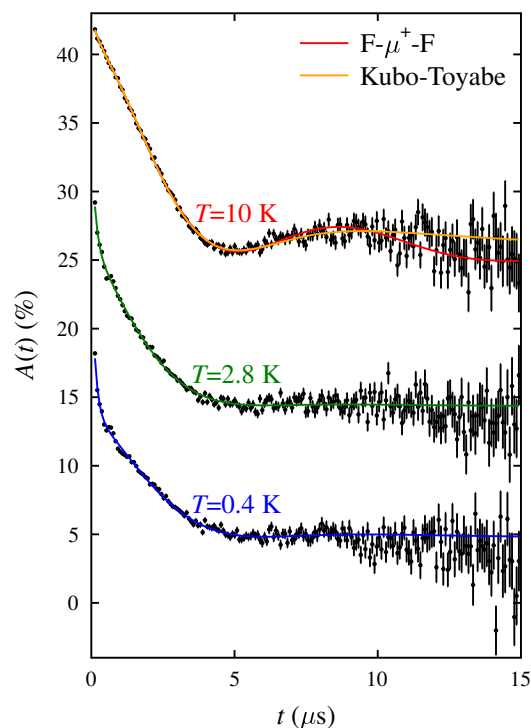


**Figure 3.** Example spectra measured on the  $Ln=Sm$  material at three different temperatures. [Spectra offset for clarity by  $A(t) + 10\%$  for  $T = 10$  K and  $T = 2.8$  K.] Lines are fits explained in the text.

to the muon. (Numerical simulations of dipole-dipole interactions are consistent with this scenario and contrasts with the case of relaxation from a dilute array of moments, which gives rise to a Lorentzian relaxation [24].) Given the presence of (electronegative) fluorine in the hfac groups, muon sites in their vicinity might be expected, while the chemical complexity of the material makes it plausible that the muon spin will also be relaxed by coupling to other nuclei in its vicinity.

In addition to the relaxation from nuclear spins, a rapidly relaxing component (with relaxation rate  $\lambda_2$ ) is observed at early times which becomes steadily more prominent as the temperature is lowered. As a result, we fit the data to a function of the form

$$A(t) = A_{\text{rel}}[p_1 e^{-\lambda_1 t} D(t) + p_2 e^{-\lambda_2 t}] + A_{\text{bg}}, \quad (6)$$

where  $D(t)$  models the muon coupling to the local nuclei,  $\lambda_i$  are relaxation rates and  $p_i$  give the proportion of the signal arising from each component. In addition to the relaxing asymmetry  $A_{\text{rel}}$  there is also a contribution  $A_{\text{bg}}$  from those muons that do not relax, including those that implant in the sizeable sample holder. We first fitted the high temperature spectra to a  $F-\mu^+-F$  model [17] (Fig. 3, red line) and obtained a characteristic frequency  $\omega/2\pi = 0.046$  MHz, corresponding to large  $\mu^+-F$  distances of  $r \approx 2.0$  Å. These spectra are also well captured by a KT model (Fig. 3, orange line) with  $\Delta = 0.34 \mu\text{s}^{-1}$ , which is fairly typical for relaxation due to nuclear moments in the paramagnetic regime of a molecular material. As the  $\mu^+-F$  distance required by



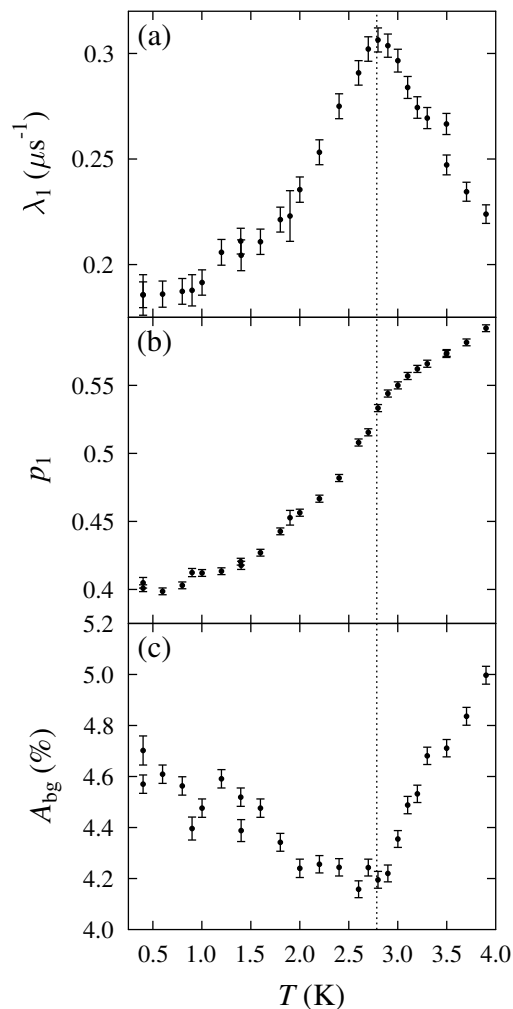


**Figure 4.** Fitted parameters from fits to Eqn (6) for the  $Ln = \text{Sm}$  material. (a) Slow relaxation rate  $\lambda_1$ , (b) slow relaxing proportion  $p_1$  and (c) baseline contribution  $A_{\text{bg}}$ .

the  $\text{F}-\mu^+-\text{F}$  model is unusually large compared to the typical bond length of  $\approx 1.1 \text{ \AA}$ , the low temperature data were fitted to Eqn (6) with  $D(t)$  described by the KT model, with the field width fixed to its average value  $\Delta = 0.29 \mu\text{s}^{-1}$ . The relaxing amplitude and rapid relaxation rate in Eqn (6) were also found not to vary significantly with temperature and so were fixed to their average values  $A_{\text{rel}} = 20.1\%$ , and rapid relaxation rate  $\lambda_2 = 7.4 \mu\text{s}^{-1}$ .

The behaviour of the fitted parameters is shown in Fig. 4. A sharp peak in the smaller relaxation rate  $\lambda_1$  is seen at  $T_c = 2.8$  K [Fig. 4(a)]. This roughly coincides with the magnetic ordering transition reported at  $T = 3$  K previously from magnetic susceptibility measurements [13], and so we ascribe the residual relaxation of the KT function to the fluctuations of the radical spins. Previous muon measurements made on molecular radical-based magnets have seen oscillations in the muon asymmetry accompanying transitions to long range magnetic order [25] at frequencies that can be

resolved using the pulsed muon beam as the ISIS facility. It is therefore likely that the fact that oscillations are not evident in this case reflects a more complex magnetic state below the transition temperature. In the fast fluctuation limit, we expect the relaxation rate  $\lambda_1$  to vary as  $\lambda_1 = 2\Delta^2\tau$ , where  $\Delta$  is the width of the distribution of magnetic fields ( $\Delta^2 = \gamma_\mu^2\langle B^2 \rangle$ ) and  $\tau$  is its correlation time. The peak is therefore consistent with a slowing of the radical moments as the transition is approached from above. The lack of discontinuity at the transition suggests that the moments continue to fluctuate below  $T_c$ . We also see a minimum in  $A_{bg}$  in this temperature region [Fig. 4(c)]. In addition to muons that stop outside the sample, this component also has a contribution from those muons that lie along the direction of local static fields (expected to be 1/3 of the total in a polycrystalline sample). The minimum in  $A_{bg}$  is seen at  $T_c = 2.8$  K and is consistent with slow fluctuations relaxing the largest proportion of muons at this temperature. As the temperature is reduced further, the slow recovery of  $A_{bg}$  suggests that fewer muons are relaxed by the slow dynamics, consistent with a spatially inhomogeneous freezing out of the dynamics. This is also consistent with the decrease in the proportion of muons  $p_1$  relaxed by the radical spins, which decreases smoothly as temperature is lowered.

Our data therefore show clear evidence for a bulk magnetic transition at  $T = 2.8$  K, which suggests a ratio  $T_c/|J| = 0.63$ . However, the lack of oscillations and the behaviour of the dynamic relaxation suggests that the  $Ln = Sm$  ferromagnetic transition seen previously involves significant dynamic fluctuations in the muon spin-precession time window, which is typically sensitive to correlation times of order  $\tau \approx 0.1 - 10$  ns. This is also consistent with the reported ac susceptibility measurements, where a response was noted in the out of phase component  $\chi''$  close to 3 K [13]. We might therefore speculate that the ferromagnetically ordered state likely has a finite correlation length below  $T_c$ , with fluctuations over a broad range of timescales freezing out in a spatially inhomogeneous manner as the temperature is lowered.

Also notable in this material is the fast relaxation component with relaxation rate  $\lambda_2$ . This varies very little as temperature is lowered. As such relaxation is not seen in the  $Ln = La$  material (see below) we ascribe it to relaxation from the  $Sm^{3+}$  moments, which appear to fluctuate down to the lowest measured temperature of 0.3 K. (Such low-temperature fluctuations likely involve low-energy transitions between the  ${}^6H_{5/2}$  levels of the  $Sm^{3+}$  ion's ground state, split by the crystal fields into three Kramers doublets with the potential for further splitting resulting from the local magnetic field on the ordered radical spins.) Since we constrain  $p_1 + p_2 = 1$ , we see the number of muons relaxed by these spins increases as temperature is lowered and the radical spin fluctuations are frozen out.

For measurements made on the  $Ln = La$  material, little difference is observed in the spectra in the measured temperature range  $0.1 \leq T \leq 20$  K. Example data are shown in Fig. 5(a). In this case no fast relaxing component is seen, consistent with our assignment of it being due to magnetism of the metal ion in the  $Ln = Sm$  material. There is also less structure in the slow relaxation, which is more consistent with a damped KT function, suggesting that those muons that are relaxed by the  $Sm^{3+}$  ions in the  $Ln = Sm$  material

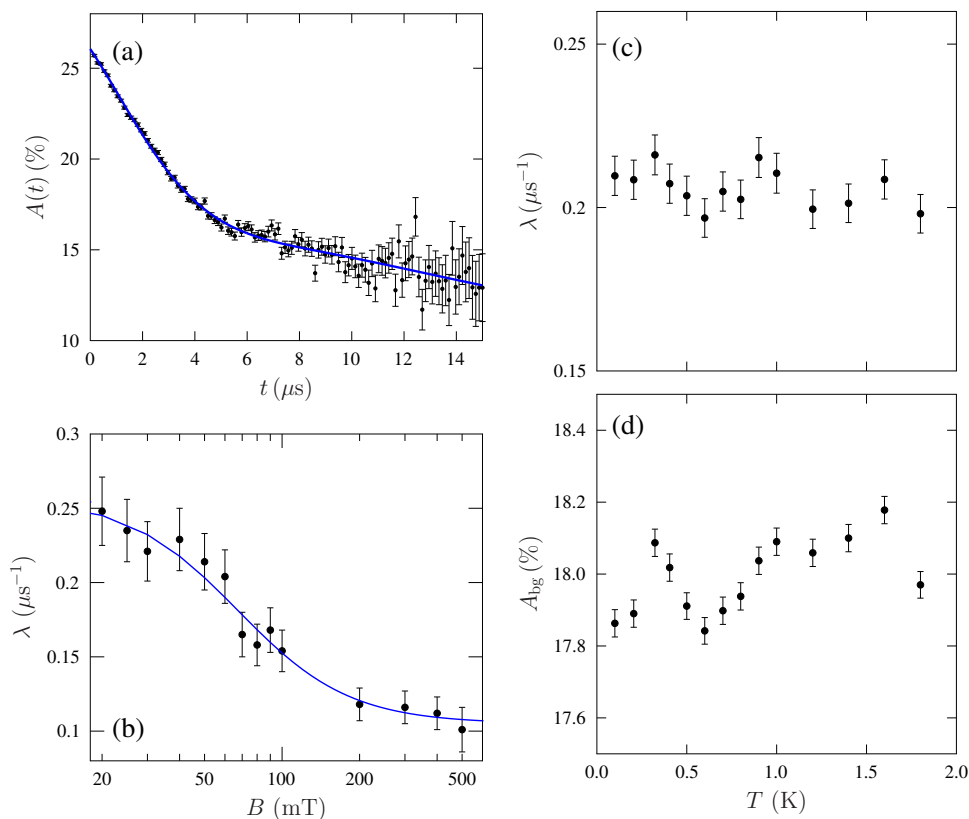


**Figure 5.** (a) Example spectra measured on the  $Ln = \text{La}$  material at  $T = 0.1$  K. (b) Longitudinal field measurements made at  $T = 1.5$  K. The blue line shows a fit to a Redfield function. (c) Relaxation rate and (d) baseline  $A_{\text{bg}}$  for fits of Eqn (7) to the data.

are relaxed by nuclei (and residual radical spin fluctuations) in the  $Ln = \text{La}$  material, leading to a broader distribution of magnetic fields at the muon site. We fitted the data with the function

$$A(t) = A_{\text{rel}} e^{-\lambda t} D(t) + A_{\text{bg}}, \quad (7)$$

where  $D(t)$  is the Kubo-Toyabe function with  $\Delta = 0.24 \mu\text{s}^{-1}$ .

As we do not see an appreciable change in relaxation over the measured temperature range [Fig. 5(c)], it is unlikely that there is any magnetic transition in the measured temperature range. This would suggest that  $T_c/|J| < 0.17$ , making this a potentially successful realization of a 1D ferromagnetic chain material [26]. There is a subtle change in the apparent background  $A_{\text{bg}}$ , as shown in Fig. 5(d), where we see that  $A_{\text{bg}}$  decreases below 1 K reaching a minimum at around 0.6 K, and a local maximum at 0.3 K. The size of these variations is small, but as they take place around the energy scale of the exchange constant  $J$  and so might reflect freezing of relaxation channels of individual spins. However, our main result is that, unlike for the  $Ln = \text{Sm}$  material, there is not evidence for collective ordering of the magnetic radical spins.

In order to gain further insight into the magnetism in the disordered  $Ln=La$  material, measurements were made as a function of magnetic field, applied longitudinal to the initial muon spin direction. The relaxation rates as a function of applied field  $B$  at fixed temperature  $T = 1.5$  K are shown in Fig. 5(b). At this temperature ( $T \gg |J|$ ) we would expect the excitations to be single spin flips. The data are well described by a Redfield model for which  $\lambda = \Delta^2\tau/[1 + (\gamma_\mu B\tau)^2]$  [27], appropriate for a dense array of dynamically fluctuating spins, with a characteristic fluctuation time  $\tau \approx 35$  ns and a field width of  $\Delta/\gamma_\mu \approx 7$  mT (the latter being fairly typical of radical magnets probed by implanted muons [25, 28]). This is consistent with fluctuations of the radical spins, which appear to persist to the lowest measured temperatures and it is likely these parameters also describe the electronic fluctuation distribution of radical spins in the  $Ln = Sm$  material.

## 5. Conclusions

We have presented the results of muon spin relaxation measurements on two different molecular spin chain systems. In  $CuF_2(pyiz)$  we observed a transition to a regime of long-range magnetic order below  $T = 0.6(1)$  K and have shown that the system represents a reasonably successful realization of a quasi 1D Heisenberg antiferromagnet. The radical magnet system  $[Ln(hfac)_3(boaDTDA)]_n$  with  $Ln = Sm$  and  $La$  represents one of the most chemically complex magnetic systems investigated using  $\mu^+$ SR to date. We have shown that the magnetic transition in the  $Ln = Sm$  material likely represents a freezing of slow dynamics giving rise to a dynamically fluctuating and spatially inhomogeneous magnetic state for  $T < T_c$  with  $Sm^{3+}$  spins continuing to fluctuate down to the lowest temperatures. It is unclear whether the driver for these slow magnetic fluctuations is the array of  $Sm^{3+}$  spins or is related to the extended nature of the electron density distribution over the radical units that results in the McConnell coupling mechanism. We note that this is not generic behaviour for a 1D ferromagnetic chain of radical spins, as several examples have been previously studied and show conventional magnetic order at low temperature [25, 29, 26]. The  $Ln = La$  material shows no sign of magnetic order down to  $T = 0.1$  K, with the radical spins remaining in a dynamically fluctuating magnetic state.

## Acknowledgments

This work was carried out at the STFC-ISIS facility, Rutherford Appleton Laboratory, UK and we are grateful for the provision of beamtime. We thank EPSRC, UK and STFC for financial support. The Natural Science and Engineering Research Council (NSERC) of Canada supported KEP's contribution to this work through a Discovery Grant (DG). JAS acknowledges support from the Independent Research/Development (IRD) program while serving at the National Science Foundation. Research data from this publication will be made available via Durham University. (*DOI(s) will be inserted*

here.)

## References

- [1] Blundell S J 2007 *Contemp. Phys.* **48** 275
- [2] Blundell S J and Pratt F L 2004 *J. Phys.: Condens. Matter* **16** R771
- [3] Giamarchi T 2003 *Quantum Physics in One Dimension* (Oxford: OUP)
- [4] Sachdev S 2011 *Quantum Phase Transitions, second edition* (Cambridge: CUP)
- [5] We use the single- $J$  convention here where the energy gap between the singlet and triplet level of a two spin system with Hamiltonian  $\hat{H} = J\hat{\mathbf{S}}_i \cdot \hat{\mathbf{S}}_j$  is given by  $J$ .
- [6] Blundell S J, Lancaster T, Pratt F L, Baker P J, Brooks M L, Baines C, Manson J L and Landee C P 2007 *J. Phys. Chem. Solids* **68** 2039
- [7] Sengupta P, Sandvik A W, and Singh R R P 2003 *Phys. Rev. B* **68** 094423
- [8] Schulz H J 1996 *Phys. Rev. Lett.* **77** 2790
- [9] Lancaster T, Blundell S J, Pratt F L 2013 *Physica Scripta* **88** 068506
- [10] Huddart, B M, Brambleby J, Lancaster T, Goddard P A, Xiao F, Blundell S J, Pratt F L, Singleton J, Macchi P, Scatena R, Barton A M and Manson J L 2019 *Phys. Chem. Chem. Phys.* **21** 1014
- [11] Lapidus S H, Manson J L, Liu J, Smith M J, Goddard P A G, Bendix J, Topping C V, Singleton J, Dunmars C, Mitchell J F, and Schlueter J A 2013 *Chem. Commun.* **49** 3558
- [12] Fatila E M, Clérac R, Rouzières M, Soldatov D M, Jennings M and Preuss K E 2013 *Chem. Commun.* **49** 6271
- [13] Fatila E M, Maahs A C, Mills M B, Rouzières M, Soldatov D M, Clérac R and Preuss K E 2016 *Chem. Commun.* **52** 5414
- [14] Blundell S J 1999 *Contemp. Phys.* **40**, 175
- [15] Butcher R T, Landee C P, Turnbull M M and Xiao F 2008 *Inorg. Chim. Acta* **361** 3654
- [16] Lancaster T, Blundell S J, Pratt F L, Brooks M L, Manson J L, Brechin E K, Cadiou C, Low D, McInnes E J L and Winpenny R E P, 2004 *J. Phys. Condens. Matter* **16** S4563
- [17] Brewer J H, Kreitzman S R, Noakes D R, Ansaldo E J, Harshman D R and Keitel R 1986 *Phys. Rev. B* **33** 7813
- [18] Möller J S, Ceresoli D, Lancaster T, Marzari N, and Blundell S J 2013 *Phys. Rev. B* **87** 121108(R)
- [19] Lancaster T, Blundell S J, Baker P J, Hayes W, Pratt F L, Manson J L, Conner M M Schlueter J A 2007 *Phys. Rev. Lett* **99** 267601
- [20] Steele A J, Lancaster T, Blundell S J, Baker P J, Pratt F L, Baines C, Conner M M, Southerland H I, Manson J L and Schlueter J A 2011 *Phys. Rev. B* **84** 064412
- [21] Xiao F, Möller J S, Lancaster T, Williams R C, Pratt F L, Blundell S J, Ceresoli D, Barton A M and Manson J L 2015 *Phys. Rev. B* **91**, 144417
- [22] Yasuda C, Todo S, Hukushima K, Alet F, Keller M, Troyer M, and Takayama H 2005 *Phys. Rev. Lett.* **94** 217201
- [23] McConnell H M, 1963 *J. Chem. Phys.* **39** 1910
- [24] Uemura Y J, Yamazaki T, Harshman D R, Senba M, and Ansaldo E J 1985 *Phys. Rev. B* **31**, 546
- [25] Blundell S J, Marshall I M, Lovett B W, Pratt F L, Hayes W, Kurmoo M, Takagi S and Sugano T 2001 *Hyp. Interact.* **133** 169
- [26] Blundell S J, Möller J S, Lancaster T, Baker P J, Pratt F L, Seber G and Lahti P M 2013 *Phys. Rev. B* **88** 064423
- [27] Hayano R S, Uemura Y, Imazato J J, Nishida N, Yamazaki T and Kubo R, 1979 *Phys. Rev. B* **20** 850
- [28] Blundell S J, Pattenden P A, Pratt F L, Valladares R M, Sugano T and Hayes W 1995 *Europhys. Lett.* **31** 573
- [29] Sugano T, Blundell S J, Lancaster T, Pratt F L, and Mori H 2010 *Phys. Rev. B* **82** 180401